Quantifying the Non-Gaussianity of Wintertime Daily Maximum and Minimum Temperatures in the Southeast United States

Lydia Stefanova[1*], Philip Sura[1,2], Melissa Griffin[1]

[1]Center for Ocean-Atmospheric Prediction Studies, The Florida State University, Tallahasse, FL

[2]Deptartment of Earth, Ocean and Atmosphere Sciences, The Florida State University,Tallahassee, FL

* corresponding author email: *lstefanova@fsu.edu*

Submitted to J. Climate

March 16, 2012

Revised: July 24, 2012

Abstract

This paper examines the statistics of daily maximum and minimum surface air temperature at weather stations in the Southeast United States as a function of El Niño Southern Oscillation (ENSO) and Arctic Oscillation (AO) phase. A limited number of studies address how ENSO and/or AO affect United States' daily – as opposed to monthly or seasonal – temperature averages. The details of the effect of ENSO or AO on the higher order statistics for wintertime daily minimum and maximum temperatures have not been clearly documented.

Quality-controlled daily observations collected from 1960 to 2009 from 272 National Weather Service's Cooperative Observing Network stations throughout Florida, Georgia, Alabama, and South and North Carolina are used to calculate the first four statistical moments of minimum and maximum daily temperature distributions. It is found that, over the Southeast, winter minimum temperatures have higher variability than maximum temperatures, and La Niña winters have greater variability of both minimum and maximum temperatures. With the exception of Florida's peninsula, minimum temperatures are positively skewed, while maximum temperatures are negatively skewed. Stations in peninsular Florida exhibit negative skewness for both maximum and minimum temperatures. During the relatively warmer winters associated with either a La Niña or AO+, negative skewnesses are exacerbated and positive skewnesses are reduced. To a lesser extent, the converse is true of El Niño and AO-. ENSO and AO are also shown to have a statistically significant effect on the change of kurtosis of daily maximum and minimum temperatures throughout the domain.

1. Introduction

Understanding the statistical distribution of daily winter temperature extremes is of practical interest to the human endeavors in ecology, agriculture and utilities planning. This is particularly true for regions such as the southeast United States where winter hard freezes are a relatively rare and potentially catastrophic occurrence. The winter climate of the Southeast United States is strongly influenced by the phase of ENSO. During El Niño phase winters, the 300 hPa wind anomalies show an increase southwesterly flow over the Gulf of Mexico (Kennedy et al 2007) as the tropical/Pacific jet splits over North America, leading to an increased frequency of winter Gulf cyclones (Eichler and Higgins, 2006). In the southeast US, these contribute increased cloudiness (Angell and Korshover 1987, Angell 1990; Park and Leovy 2004) and frequent rains (Gershunov and Barnett 1998) to the region; as a result, the typical El Niño winter weather is wet and cool (Ropelewski and Halpert 1986,1987; Kiladis and Diaz 1989). During La Niña phase, the tropical/Pacific jet stream becomes a single zonal jet that is typically shifted northward (Smith et al 1998). The storm tracks associated with mid-latitude cyclones tend to stay north of the southeast U.S. (Eichler and Higgins 2006), limiting the amount of cold air that reaches the region; as a result, La Niña years, are generally warmer and drier in the Southeast (Ropelewski and Halpert 1986,1987; Kiladis and Diaz 1989). However, variability in the polar jet stream position can result in extreme cold outbreaks with either ENSO phase. In addition to ENSO phase, winter temperatures in the Southeast United States are strongly influenced by the Arctic Oscillation (AO)/North Atlantic Oscillation (NAO) and to some extent the Pacific/North America (PNA) teleconnections (Higgins et al 2002, Hagemeyer 2006).

While seasonal averages can be used as a helpful guideline for climate application models, intra-seasonal extremes are often a more important factor for practical consequences – a single deep freeze event in South Florida can wreck havoc on the local agriculture (Attaway 1997). Certain agricultural crops, such as citrus and vegetables, grown in portions of the southeast U.S. during the winter and early spring are highly susceptible to damage from freezing temperatures. A series of impact freezes in the 1980s, following a serious freeze in 1977, left the citrus industry in Florida reeling. Approximately one third of the state's commercial citrus trees were destroyed and the total monetary loss was in the billions of dollars (Miller 1991). Freezing temperatures also have an impact on wildlife, such as, for example, the Florida manatee. Mortality rates for manatees tend to have a strong seasonal emphasis in winter. Manatees can die from hypothermia during unusually cold winters, as they are unable to increase heat production by metabolism to counter losses to the environment (O'Shea et al 1985).

To understand the seasonal-scale risk of experiencing extreme cold/warm winter days, it is important to understand the changes in distributions of daily minimum/maximum temperatures under different large-scale regimes. Do these distributions simply shift to the left or right with ENSO or AO phase change? Atmospheric variables' statistics are not strictly Gaussian (e.g. Sura et al 2005), and daily minimum and maximum temperatures are no exception. A shift in their expected value (warmer during La Niña, colder during El Niño) does not guarantee a corresponding shift for the entire distribution. The current literature is ambiguous about the temperature extremes associated with ENSO phase. Some sources suggest that extreme cold events are more likely with El Niño (which is associated with below-normal winter temperatures) (e.g. Gershunov 1998; Higgins et al 2002), or that extreme warm events are more likely with La Niña (e.g. Wolter et al 1999). Others (e. g. Rogers and Rohli 1991; Hansen et al 1999, Smith and Sardeshmukh 2000) suggest that severe cold outbreaks may be more likely with La Niña.

Normal (Gaussian) distributions are fully described by their mean and standard deviation. For non-Gaussian distributions, higher moments need to be considered as well. The first four moments (mean, standard deviation, skewness and kurtosis) are generally sufficient to describe most atmospheric variables' distributions. Several studies have documented the non-Gaussian nature of surface air temperatures (Toth and Szentimrey 1990, Barnston 1993, Huth et al 2001, Ryoo et al 2004, Shen et al 2011). A handful of studies (Smith and Sardeshmukh 2000, Higgins et al 2002) have considered the higher (>1) statistical moments of surface temperatures in the United States under different ENSO and AO/NAO conditions. Both studies use gridded data – NCEP 2.5-degree reanalysis (Kalnay et al 1996) in the case of Sardeshmukh and Smith (2000), and 0.5-degree COOP-station-based gridded data set (Janoviak et al 1999) in the case of Higgins et al (2002) – and examined the response of daily mean surface temperatures to different large-scale climate regime forcing.

While analysis of gridded data provides useful insights, gridding tends to reduce the variance of observed temperatures (Tencer et al 2011) and is generally associated with introduction of biases in their means, especially in winter (De Gaetano and Belcher 2006) and for maximum temperatures (De Gaetano and Belcher 2006, Tencer et al 2011). The errors introduced by gridding are highly region- and method-dependent (e.g. Shen et al 2005, DeGaetano and Belcher 2006, Rupp et al 2010, Tencer et al 2011, Berrocal et al 2012) and a function of station density (Legg 2011). By its implicit smoothing, gridding filters out potentially valuable spatial detail at the local and regional scale that can be gleaned from analysis of un-gridded station data, especially near terrain features (Tencer et al 2011, Legg 2011) and coastal boundaries (De Gaetano and Belcher 2006). In addition, averaging of daily minimum and maximum surface temperatures to obtain the daily average obscures the fact that the daily minimum and maximum surface temperatures often have dissimilar PDF shapes (Barnston 1993, Shen et al 2011) and disparate responses to the large-scale climate regimes. To illustrate this point, we constructed PDFs of daily minimum (*tmin*) and maximum surface temperatures (*tmax*) for two stations in the Southeast US – Charlotte, NC (Fig 1A) and Fort Lauderdale, FL (Fig 1B) under El Niño/La Niña and AO+/AO- regimes (see Table 1 and section 2.2 for the regime definition). Such separation of *tmin* and *tmax* makes it possible to appreciate, for example, that the warming of the expected values of the daily means associated with El Niño relative to La Niña is largely attributable to changes in the PDF of *tmax* but not *tmin* for Charlotte, and to both *tmin* and *tmax* for Ft. Lauderdale. The warming associated with AO+, on the other hand, stems mostly from changes in the *tmin* distribution for Ft. Lauderdale, but is evenly contributed by *tmin* and *tmax* for Charlotte. In addition to these shift of the expected values, distinct deformations of the PDFs are evident as well.

While it is possible to produce a catalog of all stations' distributions in different phases of these large-scale oscillations, this approach is impractical for two reasons: the need for a very large number of plots – one for each temperature variable at each station in every climate regime – and the lack of depiction of large-scale patterns of variability across stations. Instead, in this study we summarize the PDFs and describe their geographical variability based on the distributions first four statistical moments. We examine station daily maximum (*tmin*) and minimum (*tmax*) temperatures, as well as the daily average (*tave*) and diurnal range (*trange*) during different ENSO and AO phases. The data and methodology used for this study are described in section 2. Results and discussion are presented in section 3, and section 4 provides a summary and concluding remarks.

2. Data and methodology

2.1 Station Temperature Data

We use quality controlled digital data from the Summary of the Day data set (DS3200 and DS3206) supplied by the National Climatic Data Center (NCDC). The daily measurements of maximum and minimum temperature are provided by the National Weather Service's Cooperative Observation Program (COOP), which has reported these elements for over 100 years. Each data set contains over 8,000 active observing stations (NCDC 2008), though for the purpose of this study, stations were used from the states of Alabama, Florida, Georgia, North Carolina and South Carolina.

The observing record at each station from the five selected states is at least from 1960-2009, although some stations have data as far back as the early 1900's. For the purposes of this study, we selected only stations reporting since at least 1960. Stations that have more than five consecutive years of missing data were discarded, so that each station left met the criteria to use the multiple linear regression technique set forth by Smith (2007) to replace any missing data temperature at the station. In case of missing data for a given station, correlations between the existing time series at this reference station and surrounding stations within a 50-mile radius are computed and stations with correlations greater than 0.6 are retained for use in reconstructing the reference station's missing data. The choice of 0.6 correlation cutoff was made by Smith (2007) as a compromise between the need for high inter-station correlation and the need for sufficient number of surrounding stations to be used in the linear regression procedure. Once the useable surrounding stations have been identified, all data is de-trended and the seasonal cycle is removed before computing the multiple linear regressions to determine a residual value; that is then used replace the missing value at the reference station and the trend and seasonal cycle are then re-applied. For the present study, we use the January and February *tmin* and *tmax* between 1960 and 2009 at all 272 stations in Florida, Georgia, Alabama, North Carolina and South Carolina that satisfy the criteria above. Note that any potential concerns regarding the effects of station moves, instrumental or land-use changes during the study period are alleviated by the high degree of spatial coherence of our results.

2.2 Climate Regime Definitions

The ENSO phase (ENSO-neutral, El Niño, or La Niña) is defined based on the Multivariate ENSO Index (MEI) of Wolter and Timlin (1993), obtained from http://www.esrl.noaa.gov. The Jan-Feb MEI averages for each year between 1960 and 2009 were calculated, and the 10 years with largest positive values were designated as El Niño years; similarly, the 10 years with the largest negative values were designated as La Niña. The AO phase (AO-neutral, AO+, or AO-) is defined based on the Arctic Oscillation index obtained from http://www.cpc.ncep.noaa.gov, and a similar ranking of years was performed to determine the 10 years with the highest positive Jan-Feb average AO value, and the 10 years with strongest negative AO values. The ENSO and AO phase for Jan-Feb of the years between 1960-2009 is summarized in Table 1.

2.3 Methodology We opted for selecting exactly 10 years in each regime (El Niño, La

Niña, AO+ and AO-) in order to ensure sufficient amount of data points in each regime. Most years designated as non-neutral exceed +/- one standard deviation of the relevant index; all of them exceed +/- 0.85 standard deviations. Due to the relatively short data record, we are unable to treat the effects of ENSO and AO separately. Undoubtedly, as evident from Table 1, there is a certain degree of overlap between ENSO and AO years. We acknowledge that separate consideration of each regime combination listed in Table 1 would be ideal, had the data record been sufficiently long to populate each cell with a large number of years. However, given this data record limitation, we argue that considering ENSO and AO as independent forcings is justified based on the low correlation between the time series of the two indices (Higgins et al 2002) and the consequential fact that the both El Niño and La Niña years contain a similar number of AO+ (three vs. four) or AO- (two vs. one) years.

We analyze the first four statistical moments – mean, variance, skewness and kurtosis – of the wintertime daily air surface temperature variables (maximum, minimum, average, and range) for stations in the Southeast United States under different large-scale climate regimes. As a first step, the seasonal cycle is removed from the data set, *i.e.*, climatological values for each date are calculated and subtracted from each data point. Further work is shown in terms of the resulting anomalies.

The statistical moments are defined as follows. The mean of a station variable x is calculated as $\overline{x_R} = \frac{1}{nN_R}\sum_{year \in R}\sum_{day=1Jan}^{28Feb} x(year, day)$. Here R is a given regime (one of: ENSO-neutral, El Niño, La Niña, AO-neutral, AO+ or AO-), N_R is the number of years in the dataset that fall within the selected regime, R and n is the number of days between 1 January and 28 February (i.e., 58). The corresponding standard deviation is given by

$\sigma_R = \sqrt{\frac{1}{nN_R} \sum_{year \in R} \sum_{day=1Jan}^{28Feb} \left(x(year, day) - \overline{x_R} \right)^2}$. Variance, the second statistical moment, is defined as the square of the standard deviation. In the remainder of the text for simplicity we discuss the standard deviation instead of the variance.

Skewness is a measure of the asymmetry of the distribution. It is defined as $s_R = \frac{1}{nN_R} \sum_{year \in R} \sum_{day=1Jan}^{28Feb} \left(\frac{x(year, day) - \overline{x_R}}{\sigma_R} \right)^3$. For a Gaussian variable s_R is zero. Negative (positive) s_R describes a distribution for which the left (right) tail is longer than the right (left) and whose mean value is smaller (larger) than its median value.

Kurtosis is a measure of the sharpness of the distribution. It is defined as $k_R = \frac{1}{nN_R} \sum_{year \in R} \sum_{day=1Jan}^{28Feb} \left(\frac{x(year, day) - \overline{x_R}}{\sigma_R} \right)^4$. For a Gaussian variable k_R is 3. Excess kurtosis is defined as $k_R - 3$. Negative (positive) excess kurtosis describes a distribution that is flatter (sharper) than the normal distribution, and whose tails are lighter (heavier).

2.4 Error and Significance Estimation

To correctly quantify the non-Gaussianity of temperature data we also need to specify the statistical errors we expect in our skewness and kurtosis estimates. The exact standard errors (remember that approximately 68%/95%/99% of close-to-Gaussian data can be found between ±1/2/3 standard errors) of skewness and kurtosis depend on their underlying distribution but can be approximated for weakly non-Gaussian data as $SE_{skew} = \sqrt{6/N_{in}}$ and $SE_{kurt} = \sqrt{24/N_{in}}$, respectively, where N_{in} is the effective number of independent observations (e.g., Brooks and Carruthers 1953). It has been shown (e.g., Perron and Sura 2012) that the formulas for SE_{skew} and SE_{kurt} are good approximations even for strongly non-Gaussian data. The standard error estimates for the mean and standard deviation can be related to the standard deviation magnitude using the expressions $SE_{mean} = \sigma_R \big/ \sqrt{N_{in}}$ and $SE_{\mathrm{var}} = \sigma_R \big/ \sqrt{2N_{in}}$.

As we are mainly interested in the non-Gaussian statistics of the temperature data, let us estimate the expected standard errors for skewness and kurtosis. For the present observational analysis we used 50 years of data (1960 – 2009). Therefore, the entire wintertime (January, February) record consists of, neglecting February 29th of leap years, 50 × 59 = 2950 days. As our climate regime definition uses the ten years with the highest/lowest ENSO and AO indices, we have 590 days in each distinct ENSO and AO climate state. Of course, the neutral states contain the remaining 30 years with 1770 days. If we now make the realistic assumption that surface air temperature has a decorrelation time scale of about 3 days all over the southeastern U.S. (Barnston, 1993), we can estimate the number of independent observations in the ENSO and AO climate regimes as $N_{in}^{regime} = 197$ (the total number of days in each regime, 590, divided by the decorrelation time scale of 3 days). In the neutral state there are $N_{in}^{neutral} = 590$ (the total number of days in the neutral condition, 1770, divided by the decorrelation time scale) independent records. Thus, the standard errors of skewness and kurtosis in each climate regime are $SE_{skew}^{regime} \approx 0.17$ and $SE_{kurt}^{regime} \approx 0.34$, respectively. The standard errors in the neutral phases, due to the larger number of independent observations, are somewhat smaller, namely $SE_{skew}^{neutral} \approx 0.1$ and $SE_{kurt}^{neutral} \approx 0.2$. As we are also interested in the skewness and kurtosis *differences* between ENSO/AO regimes and neutral phases, we use Gauss' propagation of uncertainty law to estimate the standard errors of the differences:

$$SE_{skew}^{regime-neutral} = \sqrt{(SE_{skew}^{regime})^2 + (SE_{skew}^{neutral})^2} = 0.19, \quad SE_{kurt}^{regime-neutral} = \sqrt{(SE_{kurt}^{regime})^2 + (SE_{kurt}^{neutral})^2} = 0.39.$$

In light of the following presentation and discussion of skewness and kurtosis maps, the error estimates mean that most of the non-Gaussian skewness structures we present in this paper (regimes and regime differences) are significant on the 95% level because the amplitudes of almost all the large-scale skewness features fall outside the plus/minus two-standard error range. Most of the kurtosis patterns are also significant on the 95% level, yet there are situations (i.e., variables and regions) where the significance level goes down to 68% (plus/minus one standard error). Therefore, overall we can be confident that the results shown here are not statistical artifacts but represent tangible physical phenomena.

3. Results and discussion

3.1 Neutral years

In neutral years (for brevity, in this section, these are defined with respect to ENSO; results for neutral years defined with respect to AO are nearly identical), the ***expected values*** of the distributions of the anomalies of *tmax* and *tmin* (Fig. 2 panels A[1], B[1]) and *trange* and *tave* (not shown) are all close to zero, indicating that it is unlikely that ENSO-neutral years are biased by the presence of an AO signal, despite the relatively larger number of AO- years in the ENSO-neutral regime (see Table 1). Temperatures' ***standard deviations*** (Fig. 2 panels A[2], B[2]) generally decrease southward and are smallest in the Florida peninsula (hereafter FP), with the exception of *tmin*, whose standard deviation increases westward and is relatively uniform in the north-south direction, although it is somewhat smaller in the southernmost parts of FP. The geographic distribution of ***skewness*** varies amongst the different temperature variables.

Maximum temperatures have a left (negative) skewness that increases southward, reaching the largest negative values in FP (Fig. 2, panel A[3]). In contrast, minimum temperatures are positively skewed in the non-FP part of the domain and negatively skewed in FP (Fig. 2, panel B[3]). The diurnal temperature range is weakly negatively skewed outside of FP and weakly positively skewed in FP (not shown). The daily mean temperature has negligible skewness with the exception of FP where it has pronounced negative skewness (not shown). The geographic distribution of ***excess kurtosis*** also varies among the four temperature variables. For *tmax* (Figs 2, panel A[4]) and *trange* (not shown) the excess kurtosis is increasingly negative to the north outside of FP and with some positive values in the southern portion of FP. The excess kurtosis of *tmin* (Figs 2, panel B[4]) and *tave* (not shown) is negative, with the largest values found in the Big Bend region of Florida.

The physical mechanisms responsible for the climatological structure of temperatures' first four statistical moments are quite complex and mostly beyond the scope of this study. Relevant considerations should include the climatological frequency of cloud-free skies, which increases southward (Winsberg 2003), the much stronger impact of sea surface temperatures in FP (*ibid*), and the climatological frequency and intensity of cold and warm fronts throughout the region. Cold frontal passage frequency generally decreases southward to FP (hence the larger temperature variances to the north); however, since fronts decelerate in their penetration to the south – and frequently become stationary (Hardy and Henderson 2003), the duration of frontal passage-related weather increases southward (DiMego et al. 1976). It takes a very strong – and tus infrequent – arctic front to penetrate all the way to FP, bringing very low humidities and extremely cold temperatures (Winsberg 2003) to the area (hence the increasingly negative skewness to the south). The diurnal temperature range is positively correlated with the frequency of cloudiness, precipitation and humidity (Karl et al. 1987; Leathers et al. 1998); consequently, the largest diurnal temperature ranges are found in FP (Leathers et al. 1998).

Scatter diagrams (Fig. 3) provide a summary of the differences in distribution shapes of *tmin* and *tmax* under neutral conditions. Whether the latter are defined on the basis of ENSO or AO makes little difference (compare the left and right columns of Fig. 3), which illustrates the relative robustness of the results. With the exception of Florida stations (red circles), the standard deviations of minimum and maximum temperatures are of comparable magnitudes, skewnesses are of comparable (and small, <0.5) magnitudes but of opposing sign (negative for *tmax*, positive for *tmin*), and the kurtoses are generally smaller for *tmax*. For Florida stations, on the other hand, the standard deviation of *tmin* is larger than that of *tmax*, both *tmin* and *tmax* are negatively skewed, with the left (negative) skewness of *tmin* stronger than that of *tmax*, and the kurtosis of *tmax* is larger than that of *tmin*.

3.2 ENSO phase

We find that ENSO phase has different effects on the ***expected values*** of *tmax* vs. *tmin* (Fig 4, panels A[1] and B[1] vs. Fig 4, panels C[1] and D[1]): both are warmer (relative to the neutral ENSO phase values) in La Niña winters, while El Niño cools *tmax* but has a mixed effect on *tmin* (generally cooling in FP and warming elsewhere). A likely explanation for this is that during El Niño winters there is an increased number of Gulf storms (Eichler and Higgins, 2006); the air masses associated with such storms are not particularly cold, but the increase in cloudiness (Angell et al 1990; Park and Leovy 2004) restricts daytime surface warming; this same cloudiness, however, restricts the nighttime radiative cooling. As a result of the shifts in the distributions of *tmin* and *tmax*, the diurnal temperature range increases (relative to the neutral ENSO phase values) in La Niña years and decreases in El Niño years, consistent with the relationship of diurnal temperature range and precipitation and cloudiness discussed by Karl et al. (1987) and Leathers et al. (1998). The absolute values of the temperature range change associated with La Niña are smaller than those associated with El Niño. The daily mean temperatures are increased in La Niña winters and decreased in El Niño winters, with the effect's magnitude being somewhat weaker in the latter.

The ***standard deviation*** of *tmax* and *tmin* (Fig. 4, panels A[2], B[2], C[2], D[2]) and *tave* (not shown) is increased in La Niña years and reduced in El Niño years for the northern portions of the domain, with the amplitude of the response being stronger during El Niño. Interestingly, both El Niño and La Niña years see a reduction of standard deviation for these variables over FP. The diurnal temperature range's standard deviation is not affected by the ENSO phase in any systematic way.

The magnitude of negative ***skewness*** for *tmax* is reduced in FP in El Niño years and increased in much of the domain in La Niña years (Fig. 4, panels A[3], B[3]). For *tmin* (Fig. 4, panels C[3], D[3]) the results are similar, except that the La Niña effect is more confined to FP. This is also reflected in the daily averages. The skewness of the diurnal temperature range does not respond to the ENSO phase in any systematic way (not shown).

The north-south gradient of the ***kurtosis*** of *tmax* in neutral years is exacerbated in La Niña years and reduced in El Niño years (Fig. 4, panels A[4], B[4]). The distribution of *tmin* is sharpened in the northern parts of the domain (to the point of becoming sharper-than-Gaussian) during El Niño years (Fig 4, panels C[4], D[4]). *Tmin*'s kurtosis is also increased in FP during La Niña years and decreased in El Niño years. The kurtosis of *trange* is generally reduced in El Niño years and not systematically affected in La Niña years (not shown). In La Niña years, the behavior of *tave*'s kurtosis is similar to that of *tmin*, while in El Niño years it is similar to that of *tmax*. In terms of absolute values, El Niño affects the kurtoses of *tmin* and *tave* more than La Niña does.

3.3 AO phase

The ***expected values*** of *tmax*, *tmin* (Fig. 5, panels A[1], B[1], C[1], D[1]), *trange* and *tave* (not shown) are increased in AO+ and decreased in AO-, the latter with the exception of *trange*, which does not have a uniform response to AO-. The ***standard deviations*** of *tmax*, *tmin* (Fig. 5, panels B[2] and C[2]) and *tave* are decreased in AO+ and increased in AO- (with the exception of FP, where the standard deviation of *tmin* is decreased in both cases). The standard deviation of *trange* does not have a uniform response to the AO phase. The ***skewness*** anomaly of *tmax* (Fig. 5, panels A[3] and B[3]) and *tave* is negative during AO+ and positive during AO-; for *tmin* (Fig. 5, panels C[3] and D[3]) and *trange*, the effect of AO phase on skewness is minimal. The *tmax* ***kurtosis*** (Fig. 5, panel A[4]) is increased in much of the domain and especially in Florida during AO+. During AO- (Fig. 5, panel B[4]), stations further north exhibit increased kurtosis, while those in FP have flattened distributions. The sharpening of distributions outside Florida and flattening in FP during AO-, as well as the sharpening of distributions in FP is also seen in *tmin* (Fig. 5, panels C[4] and D[4]), *trange* and *tave*.

3.4 Discussion

The warmest winters on record are frequently – but not always – associated with either a positive AO phase or with La Niña (see years' superscripts in Table 1, indicating the ranking of the 10 warmest and coldest Jan-Feb years between 1960 and 2009 for the

Southeast US, based on data from the National Climatic Data Center (NCDC) at http://www7.ncdc.naa.gov/CDO/cdo). Similarly, the coldest years are frequently – but not always – associated with a negative AO phase or with El Niño (subscripts in Table 1). Still, forty percent of the extreme warm/cold years occur during years that are neutral with respect to both AO and ENSO.

Our results indicate that ENSO's effect on average temperatures is primarily manifested through shifts in the expected values of the daily temperature maxima. The spatial distribution of the expected value shifts is strongly reminiscent of the precipitation anomaly distribution associated with La Niña/El Niño phases, suggesting that the driving mechanism behind the *tmax* response is the corresponding decrease/increase of cloudiness which suppresses/promotes daytime radiative warming of the surface temperatures. Daily minimum temperatures are affected to a lesser degree, suggesting that the El Niño-related increase in cloudiness promotes the suppression of nighttime radiational cooling that partially compensates for the cooling of daytime temperatures. In contrast, the AO effect on average temperatures is manifested through evenly matched shifts in both the minimum and maximum temperatures. This can be explained by the fact that changes in the AO phase, unlike changes in the ENSO phase, are directly related to the frequency of high-latitude frontal systems penetrating into the Southeast. The surface temperature changes brought about by such systems are associated with the advection into the area of very cold air instead of with cloudiness-dominated radiative effects. It should be noted, however, that despite the much stronger AO (compared to ENSO) signal in the surface temperatures in the Southeast, it is of lesser practical consequence, because the predictability of AO, unlike that of ENSO, is limited.

In addition to shifts in the expected values of the daily minimum and maximum surface temperatures, our study demonstrates that there are statistically significant large-scale changes in the higher moments of the temperature distributions that may affect the likelihood of experiencing extreme cold outbreaks. For example, in Southern Alabama and FP, La Niña winters (which are, on average, warmer than neutral) manifest increased standard deviation, increased negative skewness and increased kurtosis of daily maximum temperatures. Increased negative skewness and increased kurtosis are seen in the warm regimes (AO+ and La Niña) for both *tmin* and *tmax* in FP. These increases translate into thicker and longer left tails of the distributions and, therefore, in relatively high likelihood of experiencing temperatures significantly colder than the expected (warm) value (see Fig. 1, B[1] and B[3] for a visual illustration). The use of station (as opposed to gridded) data in the present study makes it possible to fully appreciate the statistically significant specific behavior of peninsular Florida's temperatures compared to the remainder of the Southeast.

4. Summary

Our analysis confirms that the distributions of winter daily maximum and minimum temperature anomalies are distinctly non-Gaussian. The shapes of their distributions have coherent spatial structures, with pronounced north-to-south gradients. At most stations, the PDFs of *tmin* and *tmax* have distinctly different shapes. The effects of ENSO and AO on daily min/max temperatures go beyond mere shifts in the means, but also affect the distributions' shape in a disparate, spatially coherent and statistically significant manner. The spatial distribution of the first four statistical moments for *tmin* and *tmax,* as well as a gross summary of the sign of their changes under ENSO or AO regime conditions is summarized in Table 2.

In the warm regimes (La Niña and AO+) compared to neutral, a larger effect is seen in the expected values of *tmax* than of *tmin*; magnitudes are similar between the La Niña and AO+ responses. With the exception of FP, the standard deviation of both *tmin* and *tmax* increases in La Niña, and decreases in AO+ years. In both La Niña and AO+ years *tmax* is more negatively skewed than in neutral years over most of the domain; the skewness of *tmin* is unchanged except in south Florida. Distributions of *tmax* are sharpened for most of the domain in AO+ years, and for Florida and the Gulf Coast in La Niña years. *Tmin* distributions are sharpened in South Florida for both warm regimes.

In the cold regimes (El Niño and AO-) compared to neutral, cool anomalies are seen in the expected values of *tmax* for El Niño and cold anomalies in both *tmax* and *tmin* for AO-. With the exception of Florida, the standard deviation is strongly decreased in El Niño years and slightly increased in AO- years. El Niño reduces the negative skewness of *tmin* and *tmax* in Florida; AO- increases the positive skewness of *tmax* in South Florida.

Let us end this paper with several thoughts on potential utilizations and future research. The documented values of the first four statistical moments at individual stations within each regime has the potential to be used in practical applications, such as, for example, the generation of synthetic data for agricultural crop yields or risk assessment models. To that end, future work is needed to develop a simple relationship between the distribution's statistical moments and threshold exceedance probabilities. How could that be done? It is possible to relate the first four statistical moments of a variable's distribution to the probability of exceedance of any chosen threshold values given some simple assumptions. For example, Sura and Sardeshmuhk (2008) and Sardeshmukh and Sura (2009) developed a general stochastic model (i.e., a null-hypothesis) for the non-Gaussian statistics of weather and climate variability that has been verified for various atmospheric and oceanic variables (Sura 2011)

In addition, if indeed changes in the higher moments alter the likelihoods of winter temperature extremes, the accurate representation of these moments should be an important consideration in the interpretation of climate and climate change modeling studies. A consequent question to follow up on, therefore, is the extent to which global and regional circulation models (or, for that matter, reanalyses) are indeed capable of accurately representing the higher moments of surface temperature distributions and the changes in such distributions associated with large-scale climate signals. This question is addressed in a forthcoming paper.

Acknowledgements

This work was partially supported by a grant from USDA. PS was also supported through NSF grant AGS-0903579. The authors would like to thank Dr. J. J. O'Brien and Mr. D. Zierden for useful discussions of the Southeast US climate, and two anonymous reviewers for their constructive comments that helped improve the manuscript.

References

Angell, J. K. and J. Korshover, 1987: Variability in US cloudiness and its relation to El Niño, 26, 580-584.

Angell, J. K., 1990: Variation in United States cloudiness and sunshine duration between 1950 and the drought year of 1988. J. Climate, 3, 296-308.

Attaway, J. A., 1997: A History of Florida Citrus Freezes. Florida Science Source, Inc., 368 pp.

Barnston, A. 1993: Atlas of frequency distribution, autocorrelation and cross-correlation of daily temperature and precipitation at stations in the US, 1948-1991. *NOAA Atlas*, **11**, 440pp.

Brooks, C. E. P., and N. Carruthers, 1953: *Handbook of statistical methods in meteorology*. Her Majesty's Stationery Office, London, 412 pp.

DiMego, G. J., L. F. Bosart, and G. W. Endersen, 1976: An examination of the frequency and mean conditions surrounding frontal incursions into the Gulf of Mexico and Caribbean Sea. *Mon. Wea. Rev.,* **104**, 709-718.

Eichler, T. and W. Higgins, 2006: Climatology and ENSO-related variability of North American extratropical cyclone activity. *J. Climate,* **19**, 2076-2093.

Gershunov, A., 1998: ENSO influence on intraseasonal extreme rainfall and temperature freqiencies in the contiguous United States: Implications for long-range predictability. *J. Climate,* **11**, 3192-3203.

Gershunov, A and T. Barnett, 1998: ENSO influence on intraseasonal extreme rainfall and temperature frequencies in the contiguous United States: Observations and model results. *J. Climate*, **11**, 1575-1586.

Hansen, J. W, J. W. Jones, C. F. Kiker and A. W. Hodges, 1999: El Niño-Southern

Oscillation impacts on winter vegetable production in Florida. *J. Climate*, **12**, 92-102.

Hagemeyer, B. C., 2006: ENSO, PNA and NAO scenarios for extreme storminess, rainfall and temperature variability during the Florida dry season. In: *Preprints, 18th Conference on Climate Variability and Change*, Atlanta, GA, American Meteorological Society, P2.4.

Hardy, J. W and K. G. Henderson, 2003: Cold front variability in the southern United States and the influence of atmospheric teleconnection patterns. *Phys. Geogr.*, **24**, 120-137.

Higgins, R. W., A. Letmaa, and V. E. Kousky, 2002: Relationships between climate variability and winter temperature extremes in the United States. *J. Climate*, **15**, 1555-1572.

Huth, R, J. Kysely and M Dubrovsky, 2001: Time structure of observed, GCM-simulated, downscaled, and stochastically generated temperature series. *J. Climate*, **14**, 4047–4061.

Janoviak, J. E., G. D. Bell, and M. Chelliah, 1999: A gridded data base of daily temperature maxima and minima for the conterminous United States: 1948-1993. *NCEP/Climate Prediction Center Atlas*, **6**, 50pp.

Kalnay, E., et al., 1996: The NCEP/NCAR 40-year reanalysis project, *Bull. Amer. Meteor. Soc.*, **77**, 437-471.

Karl, T. R., G. Kukla, J. Gavin, 1987: Recent temperature changes during overcast and clear skies in the United States. *J. Clim. Appl. Meteorol.*, **26**, 698-711.

Kennedy, A. J., M. L. Griffin, S. L. Morey, S. R. Smith, and J. J. O'Brien, 2007: Effects of El Niño Southern Oscillation on sea level anomalies along the Gulf of Mexico coast, *J. Geoph. Res.*, **112**, doi:10.1029/2006JC003904.

Kiladis, G. N. and H. F. Diaz, 1989: Global climatic anomalies associated with extremes in the Southern Oscillation. *J Climate,* **2**, 1069-1090.

Leathers, D. J., M. A. Palecki, D. A. Robinson, K. F. Dewey, 1998: Climatology of the daily temperature range annual cycle in the United States. *Clim Res*, **9**, 197-211.

Miller, K.A., 1991: Response of Florida citrus growers to the freezes of the 1980s, *Clim. Research*, **1**, 133-144.

O'Shea, T. J., C. A. Beck, R. K. Bonde, H. I. Kochman and D. K. Odell, 1985: An analysis of manatee mortality patterns in Florida, 1976-81. *J. Wildlife Management*, **49**, 1-11.

Park, S. and C. B. Leovy, 2004: Marine Low-Cloud Anomalies Associated with ENSO. *J. Climate*, **17**, 3448–3469.

Perron, M., and P. Sura, 2012: Climatology of non-Gaussian atmospheric statistics. *J. Climate* (in review).

Rogers, J. C. and R. V. Rohli, 1991: Florida citrus freezes and polar anticyclones in the Great Plains. *J. Climate*, **4**, 1103-1113.

Ropelewski, C. F. and M. S. Halpert, 1986: North American precipitation and temperature patterns associated with the El Niño/Southern Oscillation (ENSO). *Mon Wea Rev,* **114**, 2352-2362.

Ropelewski, C. F. and M. S. Halpert: Global and regional scale precipitation patterns associated with the El Niño/Southern Oscillation. *Mon Wea Rev,* **115**, 1606-1626.

Rupp, A. J., B. A. Bayley, S. S. P. Shen, C. K. Lee and B. S. Strachan, 2010: An error analysis for the hybrid gridding of Texas daily precipitation data. *Int. J. Climatol*,

30, 601-611.

Ryoo, S.-B., W.-T. Kwon and J.-G. Jhun, 2004: Characteristics of wintertime daily and extreme minimum temperature over South Korea. *Int. J. Climatol.*, **24**, 145-160.

Sardeshmukh, P. D., and P. Sura, 2009: Reconciling non-Gaussian climate statistics with linear dynamics. *J. Climate,* **22**, 1193-1207.

Shen, S. S. P., H. Yin, K. Cannon, A. Howard, S. Chetner, T.R. Karl, 2005: Temporal and spatial changes of the agroclimate in Alberta, Canada, from 1901 to 2002. J Appl Meteor, 44, 1090-1105.

Shen, S. S. P., A. B. Gurung, H.-S. Oh, T. Shu, D. R. Easterling, 2011: The twentieth century contiguous US temperature changes indicated by daily data and higher statistical moments. Clim Change, DOI 10.1007/s10584-011-0033-9.

Smith, C. A. and P. D. Sardeshmukh, 2000: The effect of ENSO on the intraseasonal variance of surface temperatures in winter. *Int. J. Climatol.*, **20**, 1543-1557.

Smith, R. A. 2007: Trends in maximum and minimum temperature deciles in select regions of the United States. FSU thesis. Retrieved from the FSU Dissertations and Theses database. (edt-06292007-164200).

Smith, S. R., P. M. Green, A. P. Leonardi, and J. J. O'Brien, 1998: Role of multiple-level tropospheric circulations in forcing ENSO winter precipitation anomalies, *Mon. Wea. Rev.*, **126**, 3102-3116

Sura, P., M. Newman, C. Penland, P. Sardeshmukh, 2005: Multiplicative Noise and Non-Gaussianity: A Paradigm for Atmospheric Regimes? *J. Atmos. Sci.*, **62**, 1391–1409. doi: 10.1175/JAS3408.1

Sura, P., and P.D. Sardeshmukh, 2008: A global view on non-Gaussian SST variability. *J. Phys. Oceanogr.*, **38**, 693-647.

Sura, P., 2011: A general perspective of extreme events in weather and climate. *Atm. Research,* **101**, 1-21.

Toth, Z. and T. Szentimrey, 1990: The binormal distribution: a distribution for representing asymmetrical but normal-like weather elements. *J. Climate*, **3**, 128-137.

Wolter, K., R. M. Dole, and C. A. Smith, 1999: Short-term climate extremes over the continental United States and ENSO. Part I: Seasonal temperatures. *J. Climate*, **12**, 3255-3272.

Wolter, K. and M. S. Timlin, 1993: Monitoring ENSO in COADS with a seasonally adjusted principal component index. In: *Proceedings of the 17th Climate Diagnostics Workshop*, Norman, OK, 52-57.

Table 1: Summary of the ENSO and AO phase in Jan-Feb for the years 1960-2009. A superscript in parentheses indicates an year's rank amongst the ten years with warmest Jan-Feb; a subscript in parentheses indicates an year's rank amongst the ten years with coldest Jan-Feb.

	El Niño	La Niña	ENSO-neutral
AO+	1973, 1992, 1993	1976, 1989$^{(5)}$, 2000, 2008	1975$^{(3)}$, 1990$^{(1)}$, 2002
AO-	1966$_{(10)}$, 1978	1963$_{(5)}$	1960, 1969, 1970$_{(6)}$, 1977$_{(2)}$, 1985$_{(8)}$, 1986, 2004
AO neutral	1983, 1987$_{(1)}$, 1995, 1998$^{(6)}$, 2003	1962, 1967, 1971, 1974$^{(2)}$, 1999$^{(4)}$	1961, 1964, 1965, 1968$_{(3)}$, 1972, 1979$_{(4)}$, 1980, 1981$_{(9)}$, 1982, 1984, 1988$_{(7)}$, 1991$^{(7)}$, 1994, 1996, 1997$^{(8)}$, 2001, 2005$^{(9)}$, 2006$^{(10)}$, 2007, 2009

Table 2: Summary of the first four statistical moments of daily maximum and minimum surface air temperatures for the Southeast in Jan-Feb in neutral years, and deviations from neutral years during ENSO and AO phases. A +/(-) sign indicates a positive/(negative)-valued change in the given regime relative to neutral year values. FP/NFP stands for Florida peninsula/not-Florida peninsula. Whenever a sign appears by itself, it applies to both FP and NFP. If only one of FP/NFP is mentioned, the change in the remaining region is negligible.

Regime	**Variable**	**Mean**	**Standard Deviation**	**Skewness**	**Excess Kurtosis**
Neutral	Tmax	0	decreasing southward	negative; largest magnitude in FP	negative in NFP; positive in FP
	Tmin	0	more uniform N-S gradient	positive in NFP; negative in FP	negative; most negative in Florida's Big Bend
La Niña minus neutral	Tmax	+	+ in NFP - in FP	-	+ in FP
	Tmin	+	+ in NFP - in FP	- in FP	+ in FP
El Niño	Tmax	-	-	+ in FP	- in FP

minus **neutral**	Tmin	+ in NFP - in FP	-	+ in FP	+ in NFP - in FP
AO+ **minus** **neutral**	Tmax	+	-	-	+
	Tmin	+	-	- in FP	- in NFP + in FP
AO- **minus** **neutral**	Tmax	-	+	+	+ in NFP
	Tmin	-	+	+ in FP	+ in NFP

List of Figures:

Fig. 1: PDF distributions for (A) Charlotte, NC and (B) Ft. Lauderdale, FL of winter daily *tmax* (A[1], A[2]; B[1], B[2]) and *tmin* (A[3], A[4]; B[3], B[4]) separated by ENSO phase (A[1], A[3]; B[1], B[3]) and AO phase (A[2], A[4]; B[2], B[4]). Solid black lines correspond to the warm regimes (either La Niña or AO+) and solid gray lines correspond to the cold regimes (either El Niño or AO-). Dashed lines indicate the respective expected value.

Fig. 2: Statistical moments of (A) *tmax* and (B) *tmin* during neutral years. Mean, standard deviation, skewness and excess kurtosis in subpanels [1]-[4] respectively. Horizontal color bar applies to the skewness and excess kurtosis (subpanels [3] and [4]).

Fig. 3: Relationship between the *tmin* and *tmax* standard deviation (top), skewness (middle) and kurtosis (bottom) for the neutral state defined based on ENSO (left) and AO (right). Stations in Florida are represented by red circles.

Fig. 4: Difference between the means, standard deviations, skewnesses and kurtoses (subpanels [1]-[4] respectively) of (A) *tmax* of La Niña vs. neutral years, (B) *tmax* of El Niño vs. neutral years, (C) *tmin* of La Niña vs. neutral years, and (D) *tmin* of El Niño vs. neutral years. Small color bars apply to the mean (subpanels [1]); the large color bar applies to the standard deviation, skewness and excess kurtosis (subpanels [2]-[4]).

Fig. 5: Difference between the means, standard deviations, skewnesses and kurtoses (subpanels [1]-[4] respectively) of (A) *tmax* of AO+ vs. neutral years, (B) *tmax* of AO- vs. neutral years, (C) *tmin* of AO+ vs. neutral years, and (D) *tmin* of AO- vs. neutral years. Small color bars apply to the mean (subpanels [1]); the large color bar applies to the standard deviation, skewness and excess kurtosis (subpanels [2]-[4]).

(A)

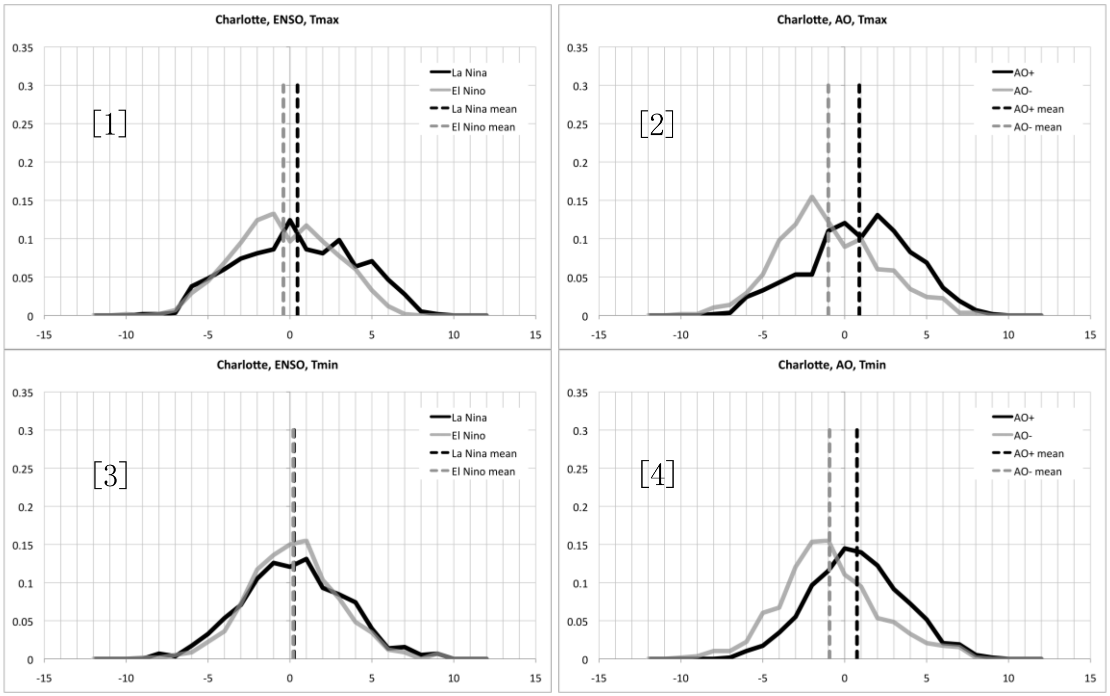

(B)

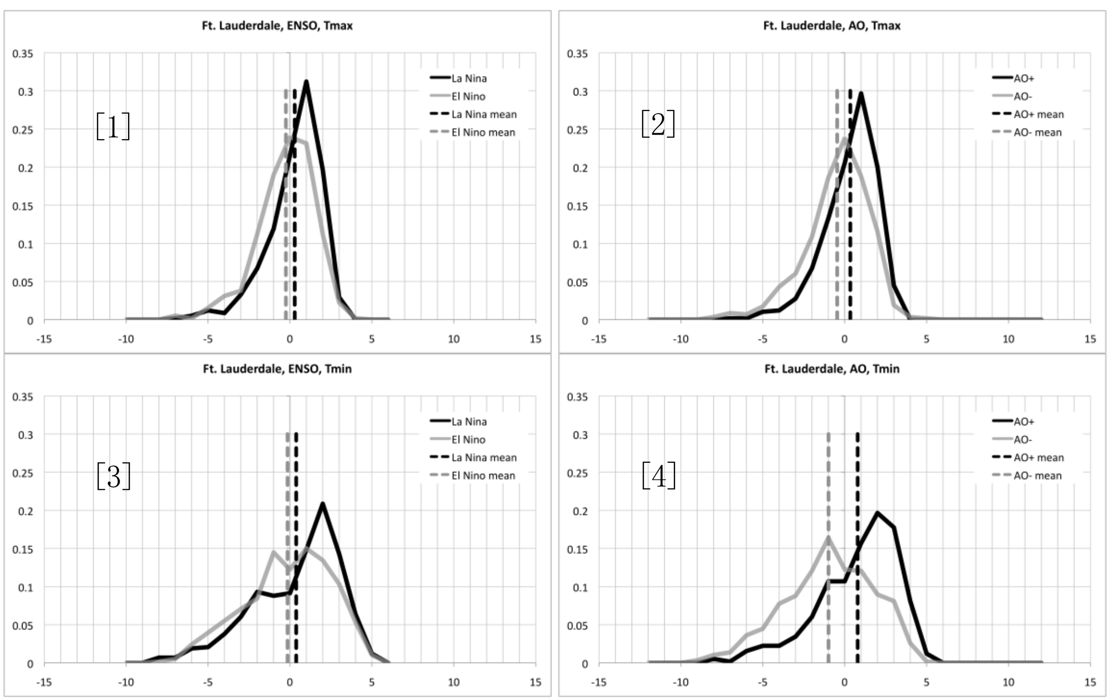

Fig. 1: PDF distributions for (A) Charlotte, NC and (B) Ft. Lauderdale, FL of winter daily *tmax* (A[1], A[2]; B[1], B[2]) and *tmin* (A[3], A[4]; B[3], B[4]) separated by ENSO phase (A[1], A[3]; B[1], B[3]) and AO phase (A[2], A[4]; B[2], B[4]). Solid black lines correspond to the warm regimes (either La Niña or AO+) and solid gray lines correspond to the cold regimes (either El Niño or AO-). Dashed lines indicate the respective expected value.

(A) *tmax*, neutral years (B) *tmin*, neutral years

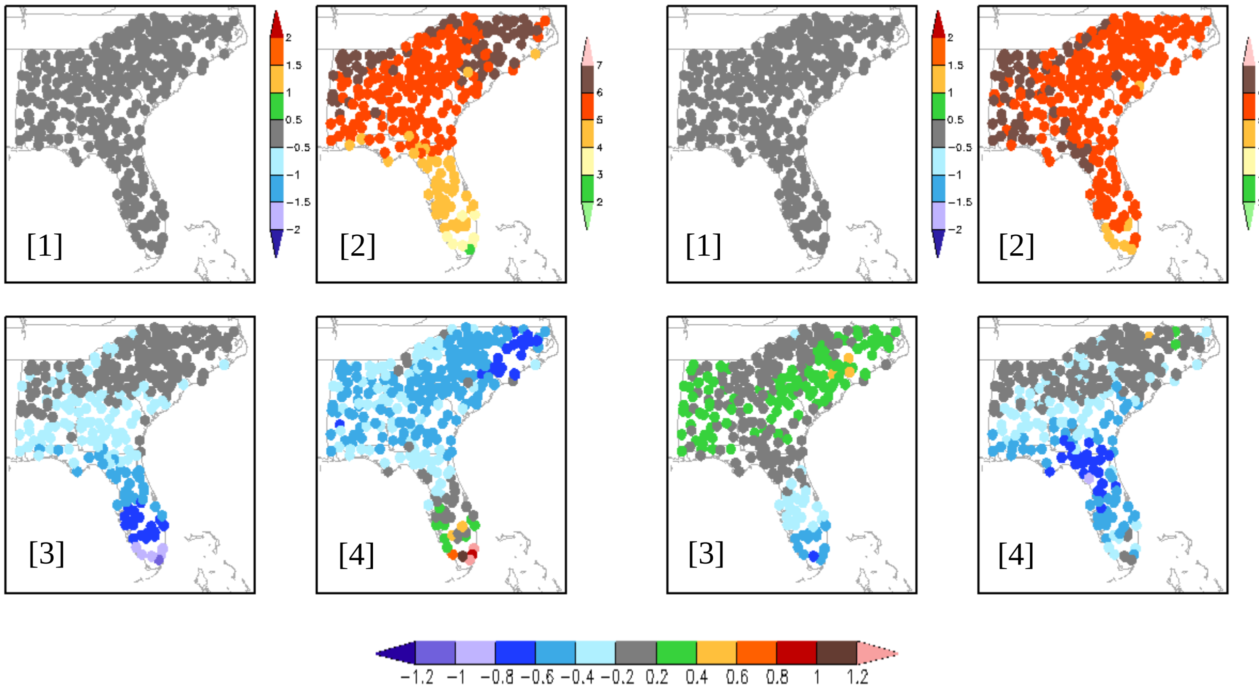

Fig. 2: Statistical moments of (A) *tmax* and (B) *tmin* during neutral years. Mean, standard deviation, skewness and excess kurtosis in subpanels [1]-[4] respectively. Horizontal color bar applies to the skewness and excess kurtosis (subpanels [3] and [4]).

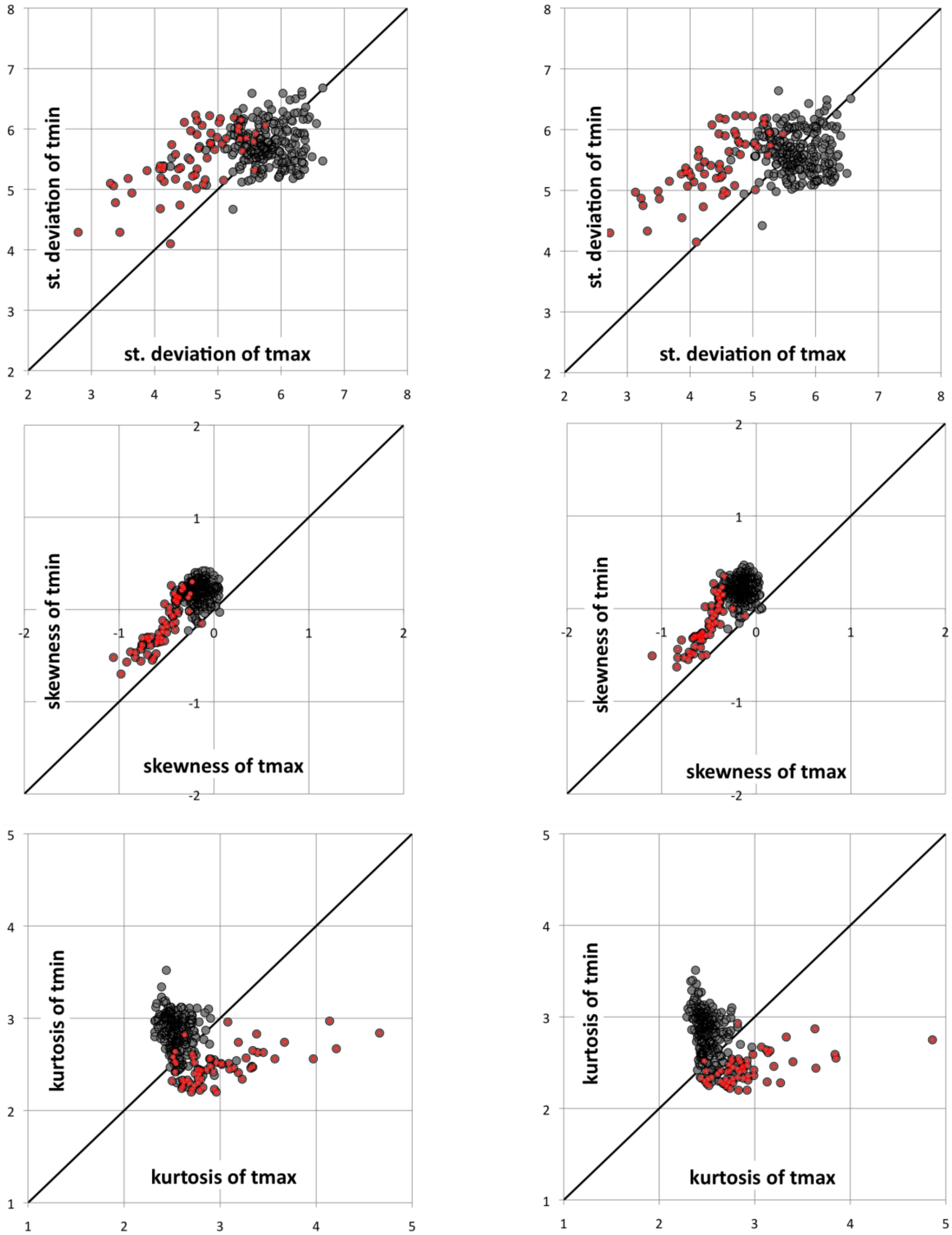

Fig. 3: Relationship between the *tmin* and *tmax* standard deviation (top), skewness (middle) and kurtosis (bottom) for the neutral state defined based on ENSO (left) and AO (right). Stations in Florida are represented by red circles.

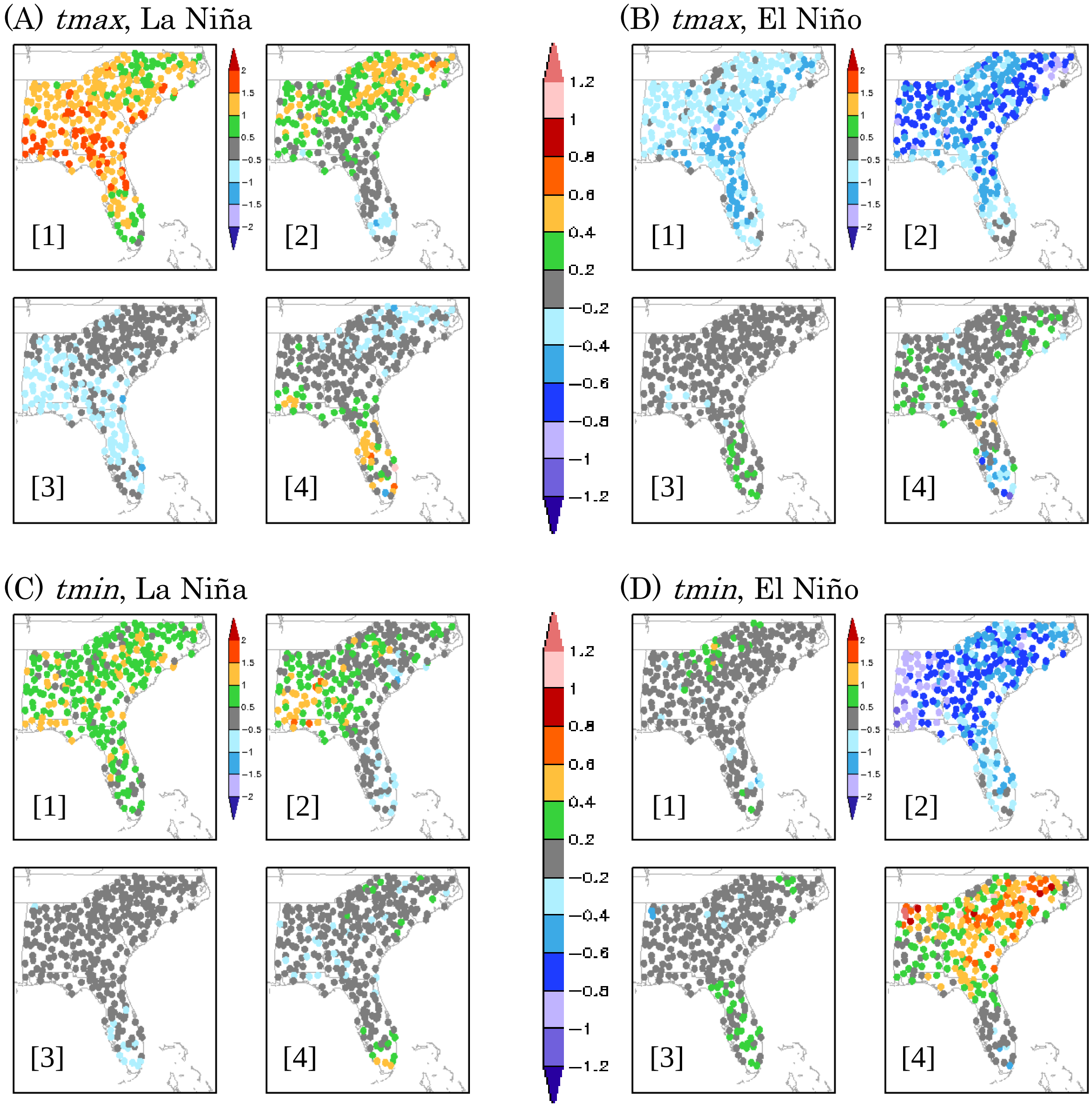

Fig. 4: Difference between the means, standard deviations, skewnesses and kurtoses (subpanels [1]-[4] respectively) of (A) *tmax* of La Niña vs. neutral years, (B) *tmax* of El Niño vs. neutral years, (C) *tmin* of La Niña vs. neutral years, and (D) *tmin* of El Niño vs. neutral years. Small color bars apply to the mean (subpanels [1]); the large color bar applies to the standard deviation, skewness and excess kurtosis (subpanels [2]-[4]).

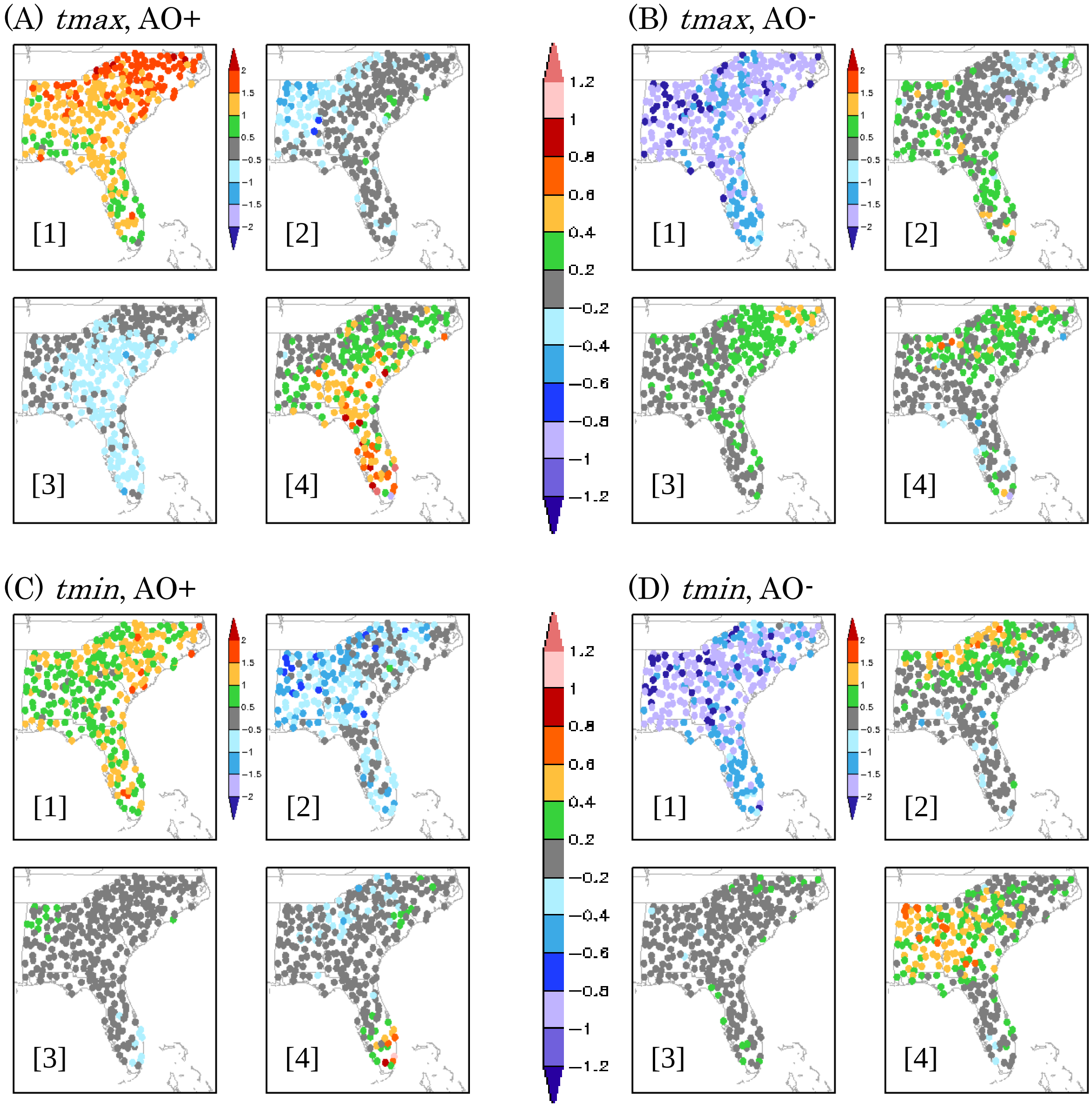

Fig. 5: Difference between the means, standard deviations, skewnesses and kurtoses (subpanels [1]-[4] respectively) of (A) *tmax* of AO+ vs. neutral years, (B) *tmax* of AO- vs. neutral years, (C) *tmin* of AO+ vs. neutral years, and (D) *tmin* of AO- vs. neutral years. Small color bars apply to the mean (subpanels [1]); the large color bar applies to the standard deviation, skewness and excess kurtosis (subpanels [2]-[4]).